AD NUMBER

B195870

NEW LIMITATION CHANGE

TO Approved for Public Release;
Distribution Unlimited.
** Stmt: A
** Code: 1

FROM

N/A

AUTHORITY

DTIC-DD, thru Chief, DTIC-OCC

L

SACLANTCEN REPORT
serial no.: SR-225

SACLANT UNDERSEA RESEARCH CENTRE

REPORT

Vertically bistatic reverberation and the back-propagated field with the split-step PE

H.G. Schneider

November 1994

The SACLANT Undersea Research Centre provides the Supreme Allied Commander Atlantic (SACLANT) with scientific and technical assistance under the terms of its NATO charter, which entered into force on 1 February 1963. Without prejudice to this main task – and under the policy direction of SACLANT – the Centre also renders scientific and technical assistance to the individual NATO nations.

Page count for SR-225
(excluding Covers
and Data Sheet)

Pages	Total
i–vi	6
1–22	22
	28

SACLANT Undersea Research Centre
Viale San Bartolomeo 400
19138 San Bartolomeo (SP), Italy

tel: 0187 540 111
fax: 0187 524 600
telex: 271148 SACENT I

NORTH ATLANTIC TREATY ORGANIZATION

SACLANTCEN SR-225

Vertically bistatic reverberation and the back-propagated field with the split-step PE

H.G. Schneider

The content of this document pertains to work performed under Project 19 of the SACLANTCEN Programme of Work. The document has been approved for release by The Director, SACLANTCEN.

David L. Bradley
Director

intentionally blank page

Vertically bistatic reverberation and the back-propagated field with the split-step PE

H.G. Schneider

Executive Summary: Since the introduction of the split-step FFT solution of the parabolic wave equation (henceforth abbreviated PE) this approach has become widely accepted as a proven and powerful tool for investigating a great variety of wave propagation problems. For underwater acoustics with rapidly changing range-dependent environmental conditions and frequencies requiring full-wave equation solutions no other modelling concept seems to be as versatile and numerically effective as the PE.

Hence it was considered worthwhile to further develop the PE at the Centre, first, by including loss due to scattering by a rough sea surface, as has been incorporated in the SAFARI and SNAP models, and second, by creating the capability to compute the reverberation from the ocean boundaries in the context of a full-wave model in a range-dependent environment. The theoretical background and some examples comparing this approach to other solutions have been documented in a previous report.

In the present document the reverberation approach is further developed covering two different aspects. The first is to allow for a vertically bistatic geometry of source and receiver where previously the source and receiver had to be co-located. The second aspect is to present the backward propagating sound field and to compare this with the reverberation. The backward propagating sound field is generally displayed as a function of depth and range while the reverberation is a function of receiver depth and arrival time.

To compute these fields two computational schemes were developed. The first propagates the scattered field from each scattering element backwards to the source and sums these contributions on a depth/range grid. This gives simultaneously the backward travelling field as well as the reverberation received at the source range for scatterers at sufficiently large distances from the source. The second scheme uses reciprocity of propagation to compute the reverberation field for arbitrary receiver depths at the source range. This scheme which is less computer intensive, but gives most of the information for practical purposes, was then incorporated into the standard PAREQ code.

intentionally blank page

Vertically bistatic reverberation and the back-propagated field with the split-step PE

H.G. Schneider

Abstract: This report continues the modelling of reverberation from the sea surface and the ocean bottom interface with the parabolic equation model PAREQ using the split-step algorithm. A previous report used the principle of propagation reciprocity to compute the reverberation for source and receivers which were co-located. Here the reverberation scheme is generalized to allow for differing depths of source and receiver, thus going from a monostatic to a 'quasi-bistatic' geometry. Additionally the full reverberant field is modelled by back-propagating the scatter contributions from the boundaries. This is done including geometrical spreading in azimuth, which requires the contributions from different ranges to be propagated independently. The back-propagated field is compared to solutions from two ray models (GSM, MOCASSIN) and displayed both as a function of range, i.e. equivalent to a transmission loss contour plot, and as a standard reverberation plot vs time.

Keywords: back-propagation ○ Generic Sonar Model ○ MOCASSIN ○ PAREQ ○ reverberation ○ vertically bistatic

Contents

1. Introduction 1
2. Description of the method 3
3. Examples 5
3.1. Single beam 5
3.2. Sea surface reverberation for a convergence zone 12
3.3. Bottom reverberation for a convergence zone profile and a seamount 17
4. Conclusion 21

References 22

1
Introduction

In an earlier report [1] a method of computing reverberation within the split-step parabolic equation model PAREQ [2] was outlined. The approach used reciprocity of propagation and was limited to a monostatic geometry, i.e. source and receiver had to be co-located. Indications were also provided of how to generalize this approach to a bistatic geometry where source and receiver are at different locations. We restrict this here to a 'quasi-bistatic' case allowing only for different depths but not for a horizontal displacement.

Two possibilities are apparent: the first again uses reciprocity of propagation, while the second one propagates the scattered field backwards in range.

To use reciprocity for a source and a receiver not at the same depth requires that two propagation runs be computed within the model, one to determine the incident sound field onto the boundaries as a function of range and the second to compute the propagation loss from all points at the boundary to the receiver, which is done by computing the loss from the receiver location to the boundary. Hence this would require only a slightly modified formulation as compared to the case of the co-located source and receiver.

The second possibility, propagating the scattered field backwards, also determines in one forward propagation run the incident field on the boundaries. Then this field is converted by the scattering integral into the backscattered field which is subsequently propagated backwards in range towards the receiver. This approach gives the reverberation solution for all possible receiver depths at the source range as well as the full backscattered field.

For the back-propagation it is important to note that the level as well as the vertical directionality of the backscattered field at the boundary is not distributed uniformly over range and azimuth, as would be the case for ambient noise created by the sea surface. Hence the mathematical treatment has a distinct difference. If the noise and receiver characteristics are independent of azimuth, then the source area at a given range from the receiver is proportional to the range r (the area is an annulus of diameter r and width dr) while the azimuthal spreading from each source area element to the receiver is $1/r$ and so these factors cancel. In that case the sound can be propagated towards the receiver in one computation run, where at each range the source contribution is added to the propagating field. This cannot be done in the case of a realistic reverberation geometry, because reverberation is certainly not isotropic and hence the contribution from each range element has to be propagated

to the receiver by an independent computation. This can become quite demanding on computer time if the ranges are sufficiently long, however, all receiver depths and ranges are covered at the same time to allow visualization of the entire back-propagating field as a function of depth and range as well as of the reverberation as a function of depth and time.

The model is thus suitable for computing reverberation for a point source and point scatterers on one track in an N×2D environment.

Other codes which include the backward propagating field, such as Collins' TWO WAY-FEPE [3], use either a two dimensional plane geometry with a line source or a cylindrical geometry with a point source. In the latter case the contribution from each reverberating surface element can be added to the backward propagating field at the appropriate range as in the noise case.

In this report some examples will be given to illustrate the reverberation field in two different ways. First as a function of range which is equivalent to a standard transmission loss display, and second as a function of time which is the standard reverberation display.

2 Description of the method

The mathematical description of the method only outlines changes to the formulation in [1]. In the split-step parabolic equation model, the complex pressure field is marched out in range, so that the field known at range r_i for all depths then serves as input to the algorithm to compute the field at range $r_i + \Delta r$. Since the total field vanishes on the pressure release sea surface, the field incident at the boundary (sea surface or bottom) is estimated by an artificial vertical array starting at the boundary and extending into the water. To achieve a good estimate, the sound speed is required to be constant over that array, otherwise errors will occur as discussed earlier [1].

The estimated incident sound intensity is denoted by $I_{\text{in}}(k, r; Z_s)$ where k is the vertical wave number, r the horizontal range to the boundary element and Z_s the source depth. I_{in} is stored at ranges $r = R_i$ and converted via the scattering integral to the backscattered field I_{out},

$$I_{\text{out}}(k, R_i; Z_s) = \int S_I(k', k)\ I_{\text{in}}(k', R_i; Z_s) dk', \tag{1}$$

where $S_I(k', k)$ denotes the backscattering function in terms of intensity.

If reciprocity of propagation is used, then the loss from the boundary element to the receiver must be known, i.e. the loss from the receiver at depth Z_r to each boundary element $I_{\text{in}}(k, R_i; Z_r)$ which requires one propagation loss run for each receiver depth Z_r.

The reverberation intensity at the receiver is

$$I_{\text{Rev}}(R_i; Z_s, Z_r) = \frac{N}{R_i^2} \int I_{\text{out}}(k, R_i; Z_s)\ I_{\text{in}}(k, R_i; Z_r) dk, \tag{2}$$

which is the analogous equation to Eqs. 10, 11 in [1], N denoting the proper normalization constant. The standard normailization of the reverberation level to a pulse length of 1 s is adopted throughout.

In this equation the reverberation intensity is a function of the range where it was generated; however, in experiments the reverberation is measured as a function of time. For source and receiver geometries, where the path lengths to the reverberation boundary element at range R_i may be approximated by that range, it may be assumed that the reverberation travel time from the source to the boundary element

at R_i and back to the receiver is given by $t_i = 2R_i/C_0$ with $C_0 = 1500$ m/s, the average sound speed. The inherent approximation is that the reverberation from range R_i arrives at the same time t_i at all receiver depths (a farfield approximation).

This scheme has been incorporated into the PAREQ standard code. For sea-surface reverberation either Lambert's rule or the wind-dependent scattering formula by Chapman and Harris [see 4] are available. In the following the scattering law is assumed to be Lambert's rule for the intensity, i.e. $S_I(k, k') = \mu\ k\ k'/k_0^2$ with k_0 denoting the acoustic wavenumber, ϕ the grazing angle, $k = k_0 \sin\phi$ and μ the Lambert constant.

For the backward propagation case the square root of the intensity $I_{out}(k, R_i; Z_s)$ is taken to be the backscattered field, where obviously no phase information is provided. This contribution is propagated backwards to the receiver at the origin, with the same forward propagation code and a properly rearranged, i.e. range-inverted, environment. For this backward propagated field two different displays are evaluated.

First the intensity fields which evolve from propagating the backscattered components backwards are added. That is, the field at range R_i contains components from all contributions starting at ranges $R_m \geq R_i$ having travelled the distance $R_m - R_i$. This summation is done for the incoherent field. This can be seen as a steady-state solution of the backward propagating field and a plot similar to propagation loss display is obtained.

Secondly, to compute the reverberation, the scattered field from R_i is back-propagated to zero range and this result is stored at time t_i for all receiver depths simultaneously. Thus a matrix of reverberation vs depth and time is built which has the restriction that the reverberation time corresponds to the experimental one only if the distance of the source and receiver to the scattering surface element is dominated by range.

3
Examples

Three examples are discussed with an increasing degree of complexity. First a simple beam with one surface contact is modelled. Secondly the reverberation from a convergence zone is evaluated, where the bottom has infinite loss. And thirdly the same CZ sound-speed profile is used with a finite-loss bottom and a seamount intersecting the propagation path.

3.1. SINGLE BEAM

The first example discussed is a Gaussian beam (from the standard PAREQ source functions) with an opening angle of 1°, which is propagated from a source at 500 m depth upwards towards the surface at an angle of 9°. The environment is isovelocity water with $C_0 = 1500$ m/s and a water depth of 1000 m. The frequency is 200 Hz corresponding to a wavelength of 7.5 m. PAREQ was run with a 1024 point FFT and a range-step size of 5 m. The array length to compute the incident field at the boundary was chosen to be 100 m which is longer than recommended in [1], because the backscatter function applied here requires a finer angular resolution than would be necessary to model Lambert's rule.

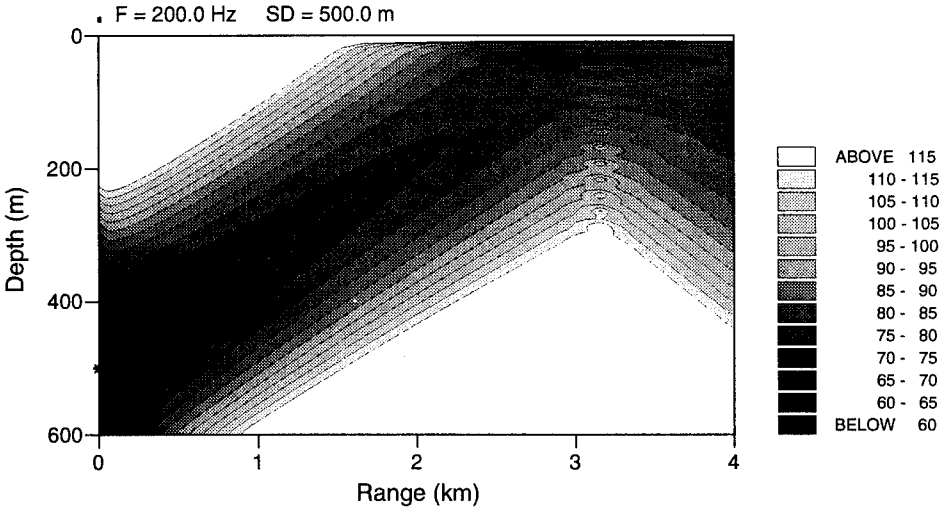

Figure 1 *Transmission loss for a Gaussian beam directed towards the sea surface, beam elevation* 9°, *Gaussian width* 1°.

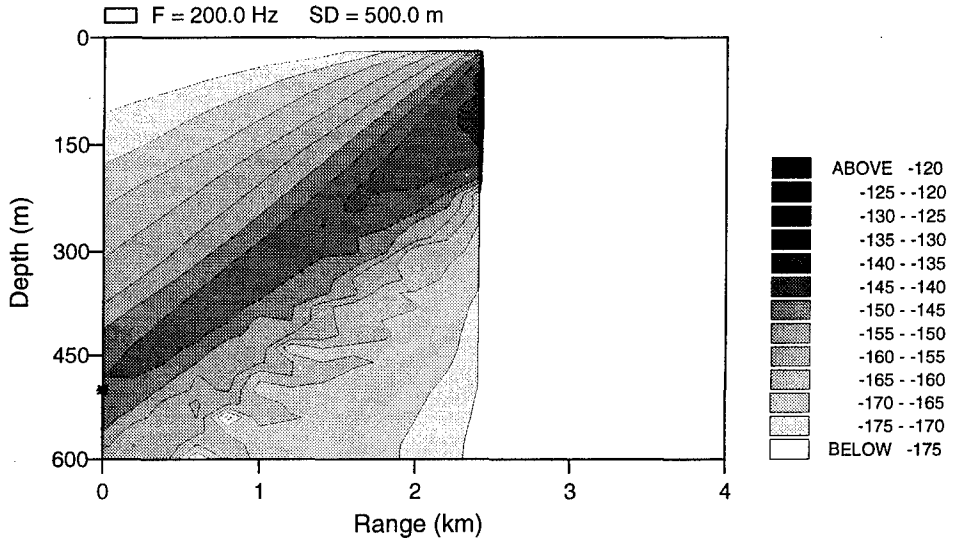

Figure 2 *Back-propagated field caused by one scattering plane (vertical array) for backscatter in the direction $-9°$ (back to the source only).*

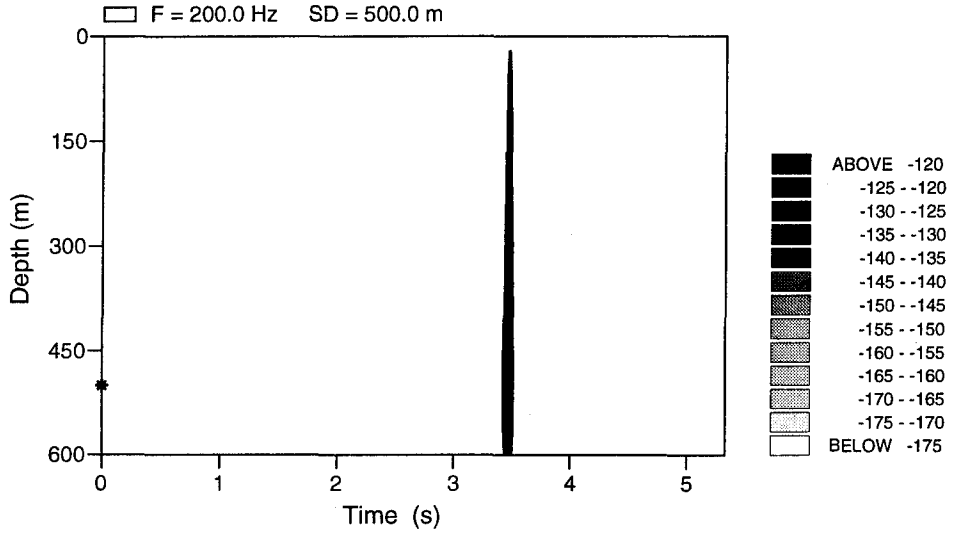

Figure 3 *Time display of the field in Fig. 2 for all receiver depths at range $r = 0$. Since the backscatter originates from one point in range it arrives (in the farfield approximation) at one time instant.*

The transmission loss including the cylindrical spreading loss is displayed in Fig. 1. Near the surface the loss is very high, however the blank area below the surface is an artifact common to this type of display program and is governed by the resolution. The spatial resolution cell is given by the small rectangle above the surface, and since the acoustic pressure is zero at the sea surface a large gradient occurs causing the first resolution cell to have this large loss. In later figures with coarser spatial resolution this will be even more apparent.

3.1.1. One backscatter direction

As a first simple test case and to familiarize the reader with the displays, it was assumed that backscatter originates at one range only and that the scatter is directed 9° downwards, that is the direction back to the source. Maintaining the scattering strength from Lambert's rule the scattering function is then $S(k, k') = \mu\ k\ k'\ \delta(k + k'\ \delta(r - R_1)/k_0^2$.

Figure 2 gives the back-propagating field as a function of depth and range as generated by one vertical source array at $R_1 = 2.6$ km with the energy distribution on the array given by I_{out}. This indicates that the array length is sufficient, the effective array length is $d_{\text{eff}} = 150$ m, to model a beam. This is like standard propagation loss contours for one source array at $R_1 = 2.6$ km range. (The display starts at 2.4 km, i.e. one output range increment of 0.2 km later, for computational convenience.) Note that the beamwidth is basically controlled by the size of the vertical array which is much smaller than the array used for the source at range zero, hence this beam is much wider than the source beam.

Figure 3 shows the same backscatter as a function of time. Since the energy originates from only one range $R_1 = 2.6$ km and range r is converted to time t by $t = 2r/C_0$ this gives only a contribution at one time instant. The width of this line is caused by using the contouring program with a coarse resolution (see resolution cell above the frame). Since the intensity distribution over depth is that at zero range in Fig. 2, the contour interpolation creates a wider line at the source depth, however the single contour lines are not resolved here, creating one black line.

Figures 4 and 5 show the corresponding results integrated over the entire sea surface. The scatter events are placed at regular intervals of 0.2 km but still assuming only one scatter direction of −9°. Figure 4 depicts the back-propagated field and Fig. 5 the reverberation. The reverberation field down to a depth of $d_{\text{eff}} = 150$ m must be considered as the 'near field' of the artificial source array and the propagation solution approximates the reverberation from the sea surface only beyond that.

Note that there is a time difference between the occurrence of the reverberation maximum in Fig. 5 and the exact solution. Ideally the centre of the source beam would hit the surface at 3.16 km resulting in a reverberation time of 4.2 s. However, the centre of the beam passes earlier (at a shorter range) through the centre of the

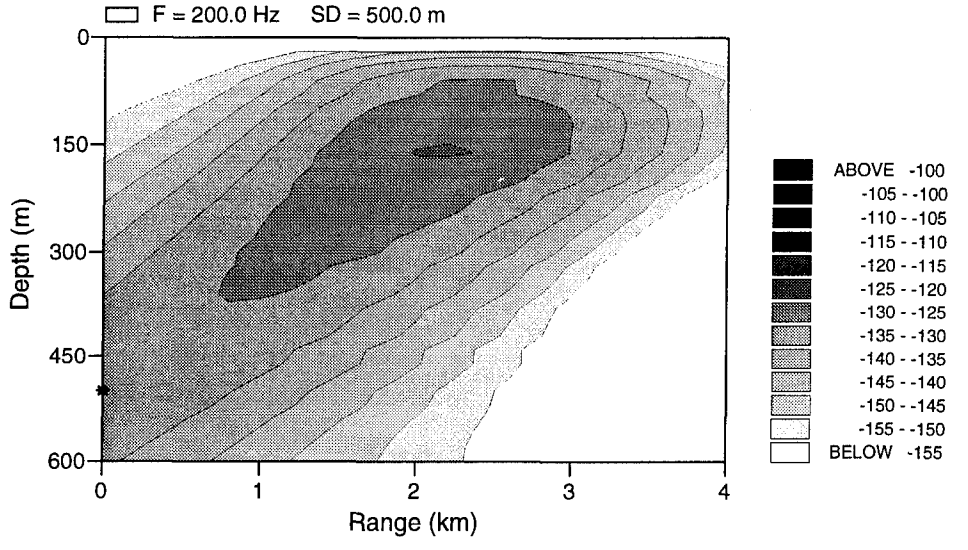

Figure 4 *Back-propagated field for backscatter in the direction −9° (back to the source only).*

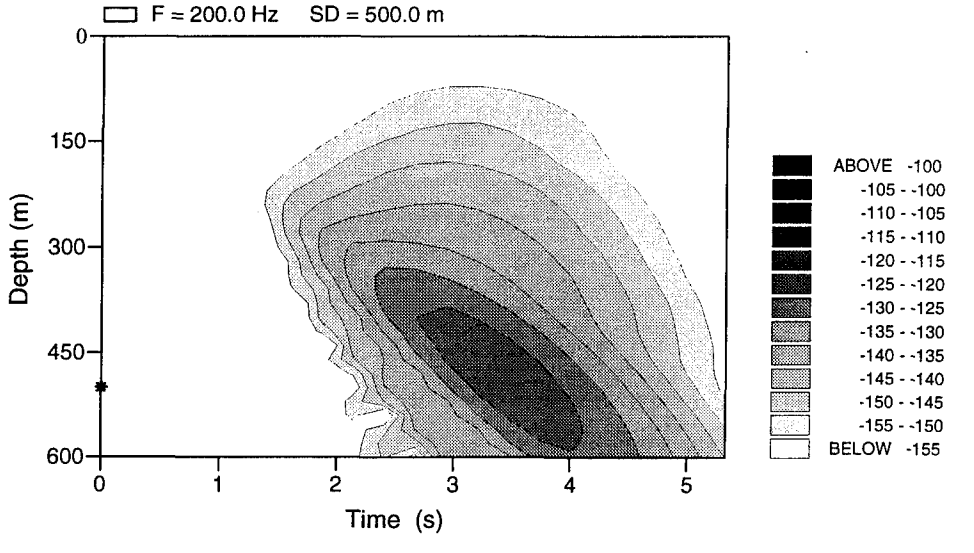

Figure 5 *Time display for all receiver depths of the field in Fig. 4 arriving at range $r = 0$.*

vertical array which is 0.5 d_{eff} below the surface. Hence the displacement corresponds to $\Delta t = \frac{2}{1500} \frac{0.5\ d_{\text{eff}}}{\tan 9^\circ} = 0.6$ s, which can be inferred from the figure.

3.1.2. Lambert backscatter

Applying the full angular dependence of Lambert's rule as a backscattering function $S(k, k') = \mu\ k\ k'/k_0^2$ gives the results shown in Figs. 6 and 7. The display of the back-propagated field vs depth and range must be considered as being integrated over time. It is, again, not valid in the depth/range region 0–150 m/1.5–3.0 km, where the beam contacts the sea surface. Outside this area it is quite clear that the scattering law directs energy mostly downwards and to a lesser extent, to shallower grazing angles. It is important here that the geometrical spreading correction has to be applied with the path length rather than the horizontal distance from the source element.

The inclination of the iso-level curves at $\sim$ 3–4 km range characterizes the limitation of the split-step propagation code in propagation angle as well as the limitation in angular resolution of the vertical array used to model the scattered energy: steeper propagation angles are not supported. A cut through Fig. 7 gives the familiar time-dependence of the backscatter at one depth which is depicted in Fig. 8 together with results using the bistatic reciprocity scheme. The source beam pattern is as given by Fig. 1. For a receiver with the characteristics of a Gaussian beam with an opening angle of 20° the reverberation levels are almost identical to the result from back-propagation where an omnidirectional receiver is assumed. This indicates that energy travelling at larger angles does not contribute significantly to the reverberation in this case.

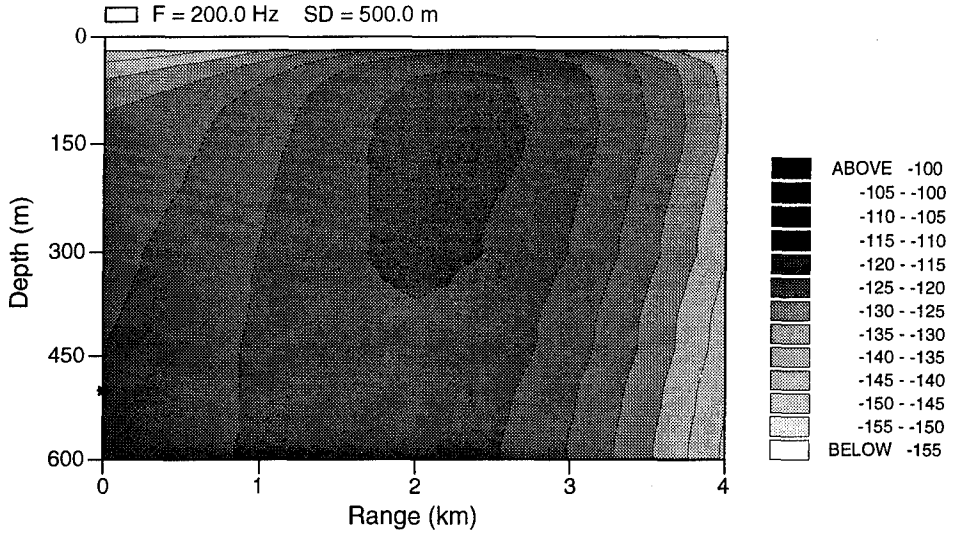

Figure 6 *Back-propagated field caused by the beam for backscatter according to Lambert's rule.*

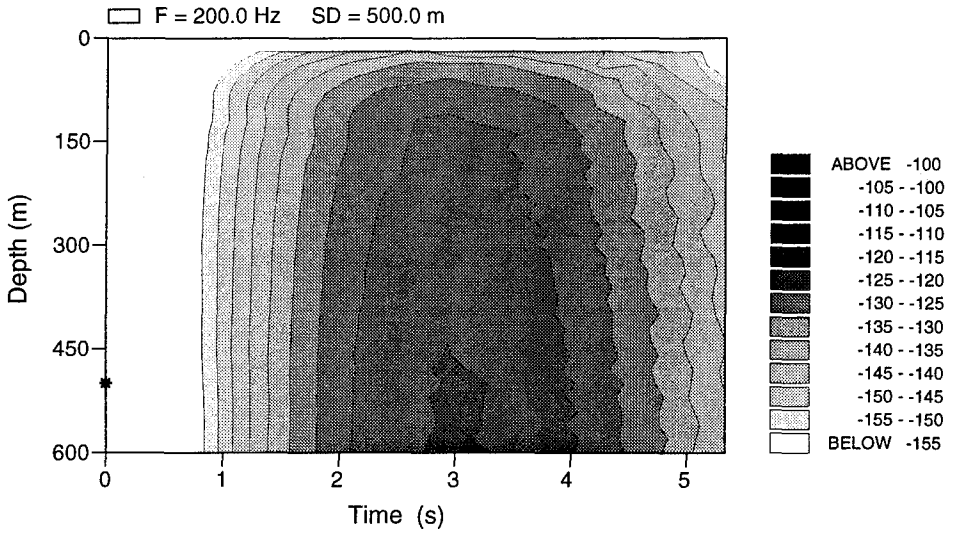

Figure 7 *Time display for all receiver depths of the field in Fig. 6 arriving at range* $r = 0$.

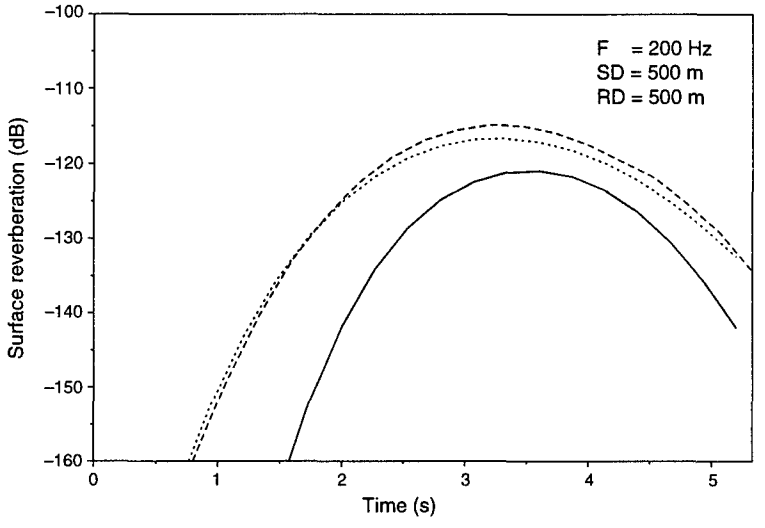

Figure 8 *Comparison of the reverberation at the source depth (500 m); solid line: reciprocity approach with narrow angle receiver; dashed line: back-propagated field with omnidirectional receiver; dotted line: reciprocity approach with wide angle receiver.*

Table 1 *Sound-speed profile for CZ propagation*

Depth	0	100	500	1000	2000	3000	m
Sound-speed	1480	1476	1470	1476	1490	1504	m/s

3.2. SEA SURFACE REVERBERATION FROM A CONVERGENCE ZONE

Next a more realistic case, namely the backscatter from the sea surface in a convergenze zone is modelled, where the bottom loss is infinite to study the reverberation from the convergence zone only. This makes the long-range propagation independent of the source characteristics, if it has a sufficiently large beamwidth. For an acoustic frequency of 100 Hz the computational parameters used for PAREQ were a 2048 size FFT, a range-step size of 20 m and a range sampling interval of 400 m for the reverberation. The sound-speed profile in the water is given in Table 1. The infinite-loss bottom was simulated by a bottom halfspace with a sound speed of 1502 m/s and a density of 1.0 g/cm^3.

Since this surface reverberation problem is easily treated by standard ray codes such as the Generic Sonar Model (GSM) [5] and MOCASSIN [6], we shall here be comparing the PAREQ wave-theory results to a set of ray solutions generated by the above models. Figure 9 shows the ray diagram from the GSM and Fig. 10 the PAREQ propagation loss contours for a source depth of 250 m and a frequency of 100 Hz.

Figures 11 and 12 display the back-propagated reverberation as a function of depth and range or time, respectively. At a first glance the difference in level between the two displays is astonishing, however, the range-dependent plot shows the steady state solution and the high reverberation levels at 30–40 km arise from the downward propagating backscatter due to the CZ encounter. Only spreading loss for a path length equal to depth occurs, while in the time display the reverberation from that range at 40–60 s includes the propagation loss from the surface encounter back to the source. (In Fig. 12 the surface reverberation for times less than 15 s, i.e. from ranges less than 11 km, and depths below 500 m, does not meet the requirement of having a path length of the order of the horizontal range, hence the reverberation times are not correct.)

Figure 13 displays the reverberation at 250 m depth computed with the reciprocity approach, the back propagation (actually a cut through Fig. 12) and the result from the Generic Sonar Model [5] with equivalent parameters.

The two PE approaches differ only slightly, most likely caused by the lack of reciprocity in using the vertical array as receiver and source, since the source field created by the array has less resolution than the original source.

Compared to the results from the GSM the reverberation from the PE is offset by 4 s. A corresponding shift would match the reverberation peaks from the CZ at 50–56 s. The correction in travel time due to the correct phase speed along the ray

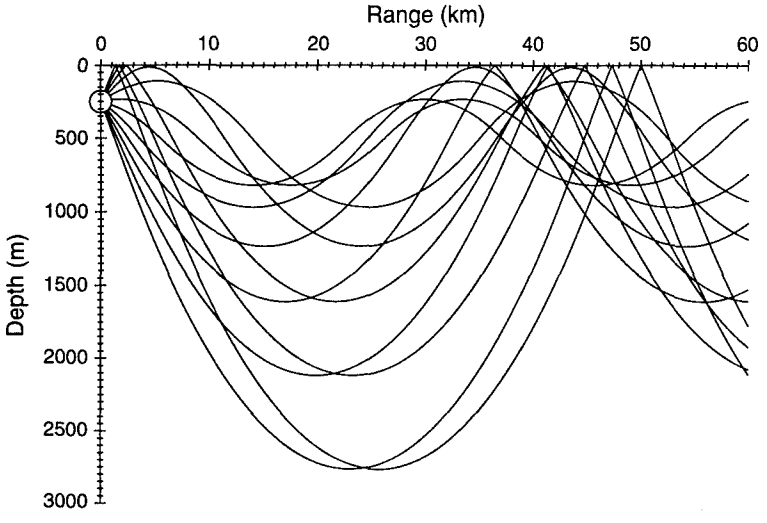

Figure 9 *Ray trace for convergence zone profile (angles from −11° to +11° with an increment of 2°) from GSM [5].*

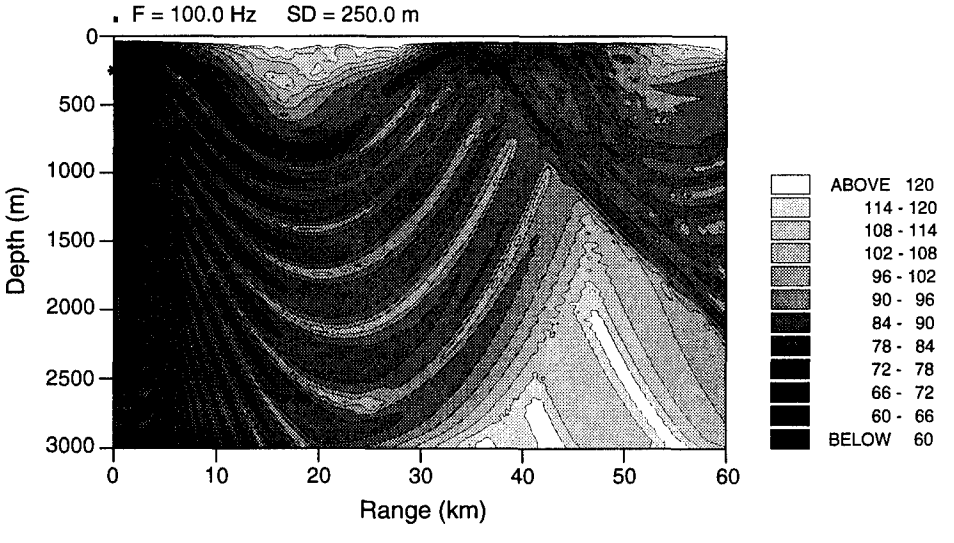

Figure 10 *Propagation loss for convergence zone profile with infinite bottom loss.*

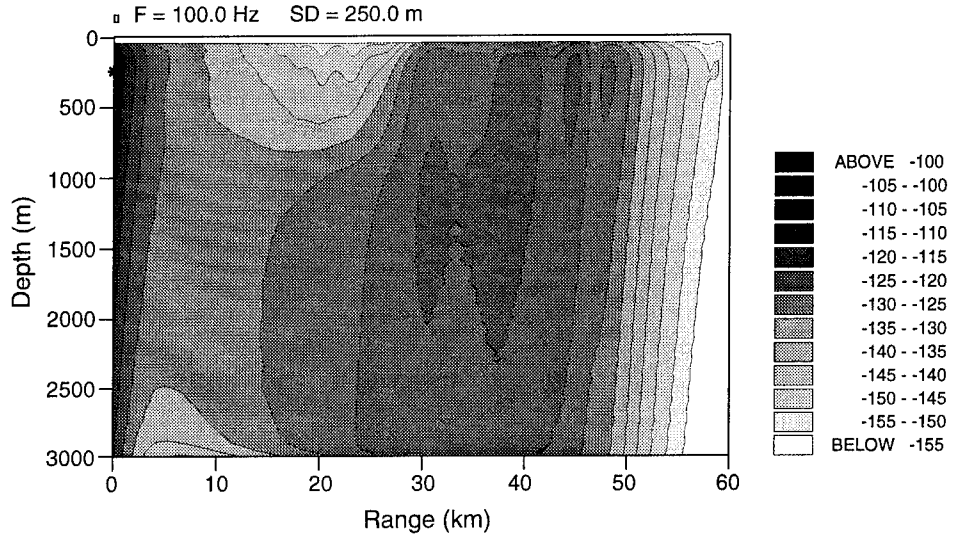

Figure 11 *Back-propagated field caused by CZ backscatter due to Lambert's rule (steady state solution).*

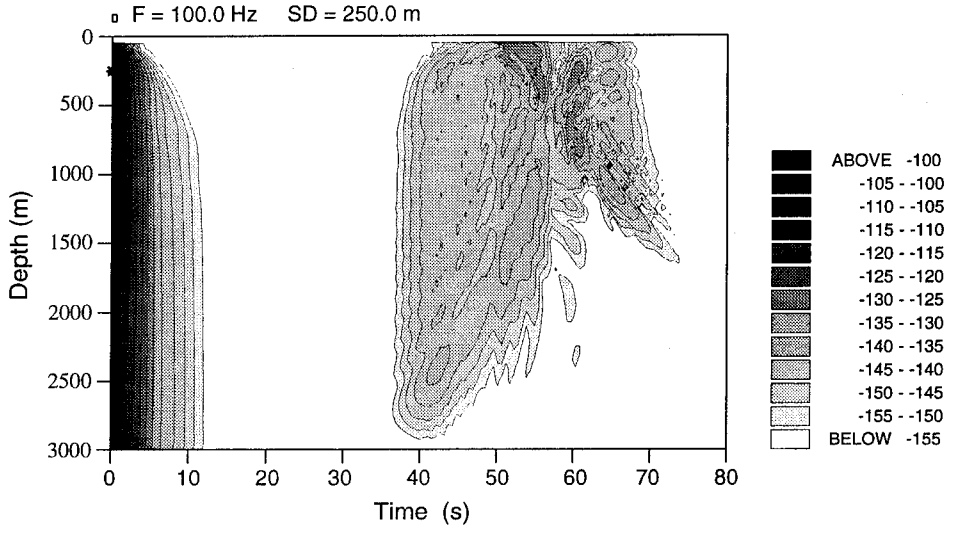

Figure 12 *Reverberation at all receiver depths caused by CZ backscatter due to Lambert's rule.*

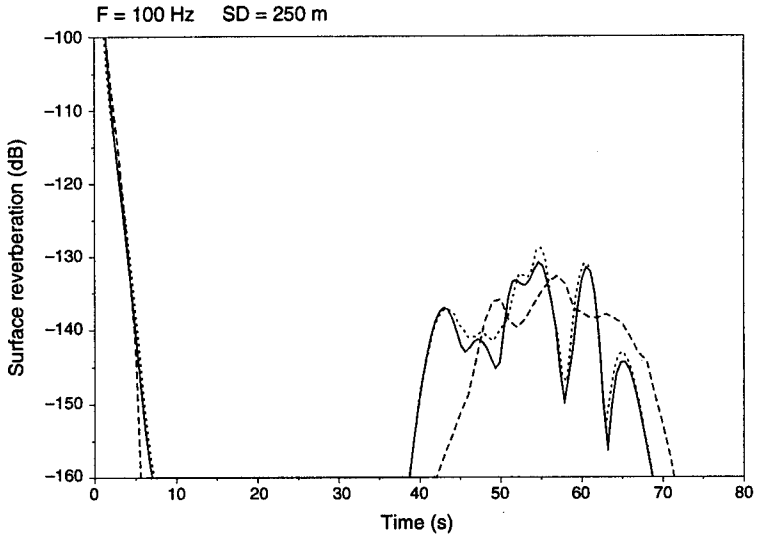

Figure 13 *Comparison of the reverberation at the source depth (250 m); solid line: reciprocity approach; dotted line: backpropagated reverberation; dashed line: from GSM.*

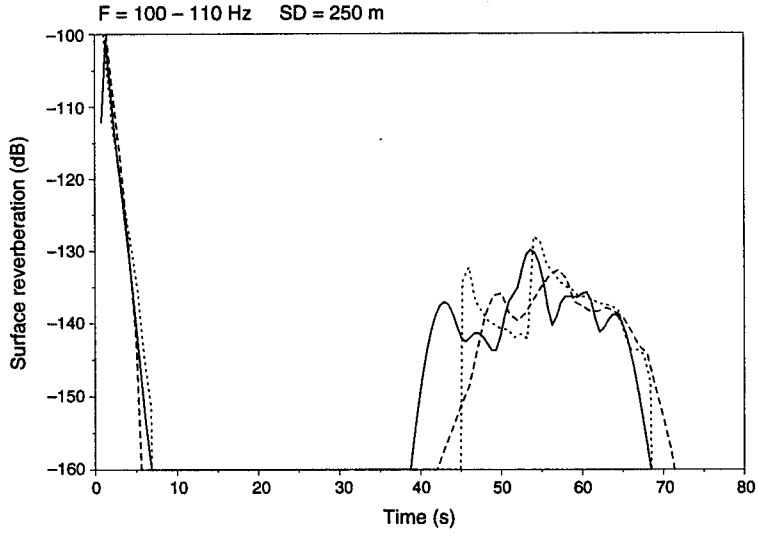

Figure 14 *Comparison of the reverberation at the source depth (250 m); solid line: 5-frequency intensity average of reverberation; dotted line: single frequency incoherent reverberation from MOCASSIN; dashed line: single frequency incoherent reverberation from GSM.*

is about 1 s in the right direction. Additional corrections arise from the fact that the incident energy is measured below the surface as explained before (Section 3.1.1).

Figure 14 shows the reverberation by averaging over 5 frequencies (100, 102.5, 105, 107.5 and 110 Hz) compared to the result from GSM and MOCASSIN [6]. The frequency averaging mainly reduces the minima and the maximum at about 60 s. Characteristically the steep onset is not smoothed or reduced. MOCASSIN computes the reverberation time t from the range r by $t = 2r/C_0$ as does PAREQ, but uses the contact on the surface. The steep onset is due to lack of wave theoretical corrections in the incoherent ray code.

The PE reverberation before the ray theoretical onset at 45 s arises from those 'rays' which propagate in the depth domain spanned by the vertical array and do not contact the sea surface, as well as by surface bounce rays with small grazing angles which are registered at the array well before they hit the surface (see ray diagram Fig. 9).

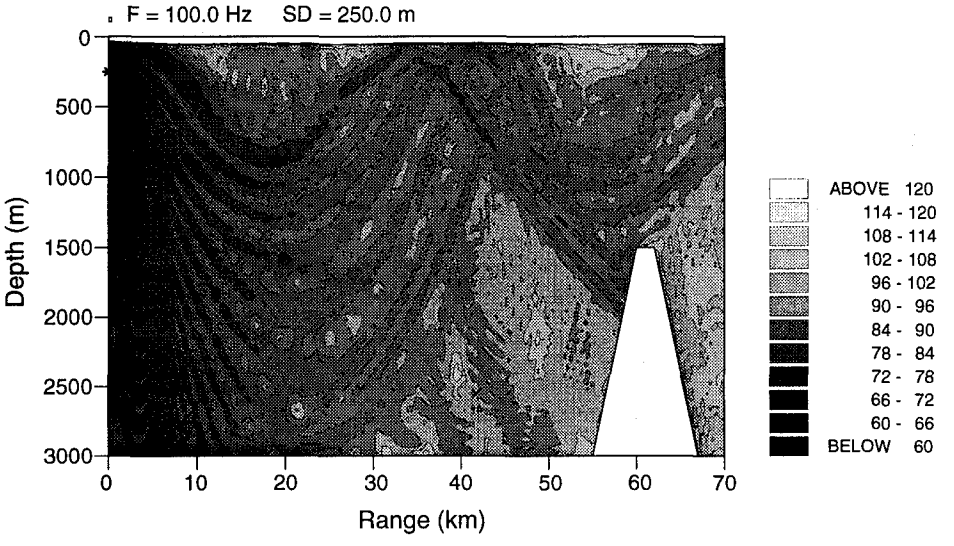

Figure 15 *Propagation loss for a convergence zone profile with a seamount.*

3.3. BOTTOM REVERBERATION DUE TO A CONVERGENCE ZONE PROFILE AND A SEAMOUNT

As a final example the same sound-speed profile is used with a reflecting bottom (half space 1600 m/s, $\rho = 1.0$ g/cm^3, $\alpha = 1.0$ dB/λ) and a seamount intersecting the propagation path. The transmission loss contours are displayed in Fig. 15.

Figure 16 shows the back-propagated field and Fig. 17 the reverberation for all receiver depths. The reverberation is received at all depths but with different levels due to propagation effects; a frequency-averaged result would bring this out more clearly.

Figure 18 gives the monostatic reverberation for 5 frequencies and also the averaged result. This is to demonstrate, as before, that with only five frequencies in a bandwidth of about 10% of the centre frequency a sufficient averaging is achieved to avoid the rapidly oscillating interference pattern. A range averaging would also smooth out the reverberation peak due to the seamount. Finally, Fig. 19 compares this average with the incoherently computed reverberation from MOCASSIN (dashed line). The peak in the bottom reverberation at 65 km or 87 s in Figs. 18 and 19 is caused by energy reflected by the seamount onto the sea surface and back to the bottom. The corresponding peak in the sea-surface reverberation occurs at 61 km in Fig. 21.

The overall agreement with MOCASSIN is better than that reported in [1], since the shallow water approximation for the reverberation in the MOCASSIN model has been changed, and is now also adequate for deep water. To see this more clearly compare the last two figures of [1] with the new version, i.e. Figs. 20 and 21.

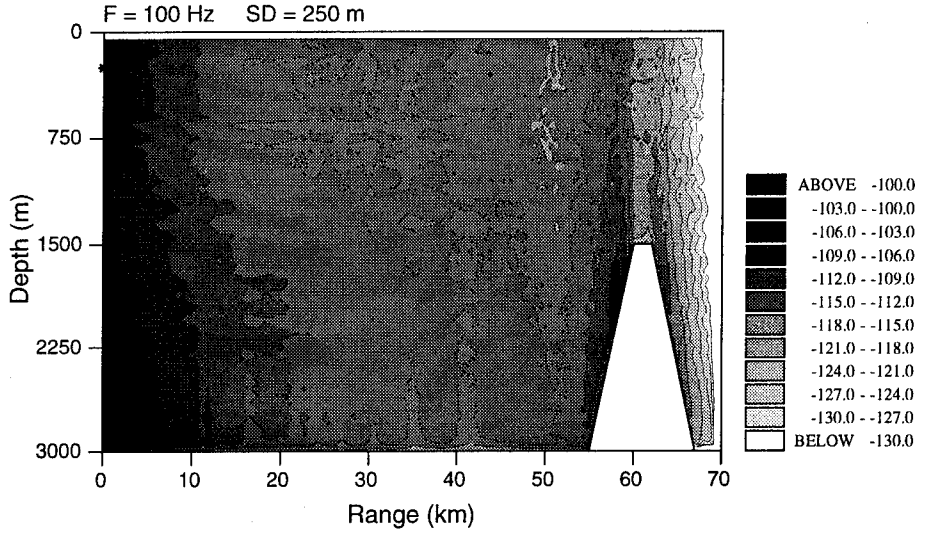

Figure 16 *Back-propagated field caused by backscatter from the bottom due to Lambert's rule (steady state solution).*

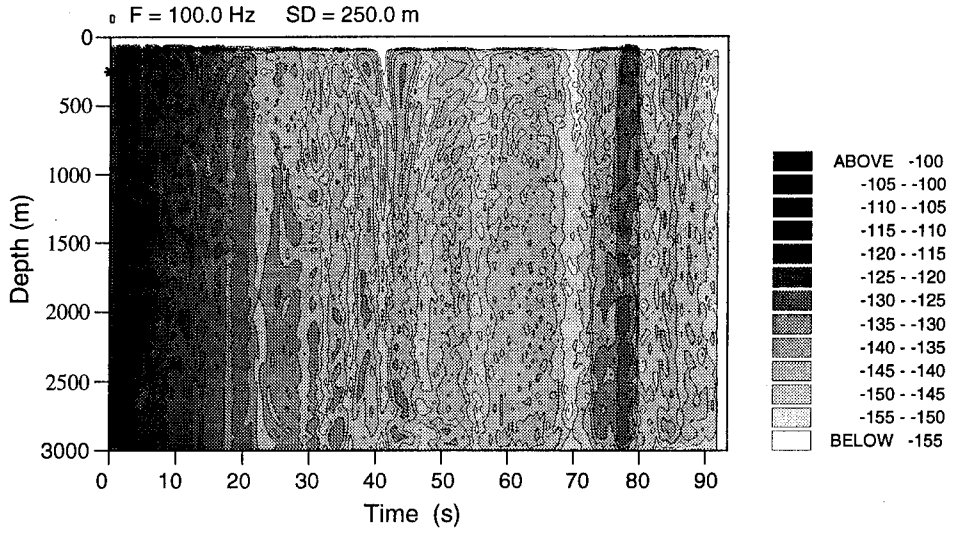

Figure 17 *Reverberation at all receiver depths caused by backscatter from the bottom due to Lambert's rule.*

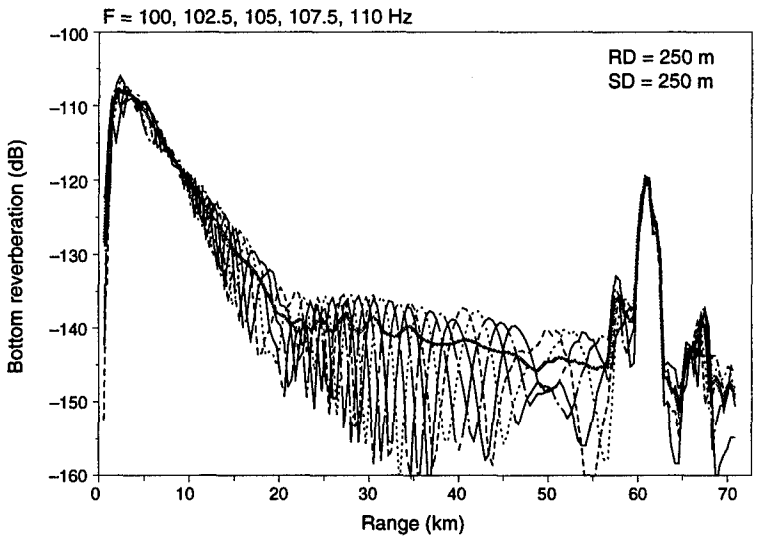

Figure 18 *Monostatic reverberation from the bottom for five frequencies and the average (heavy solid line).*

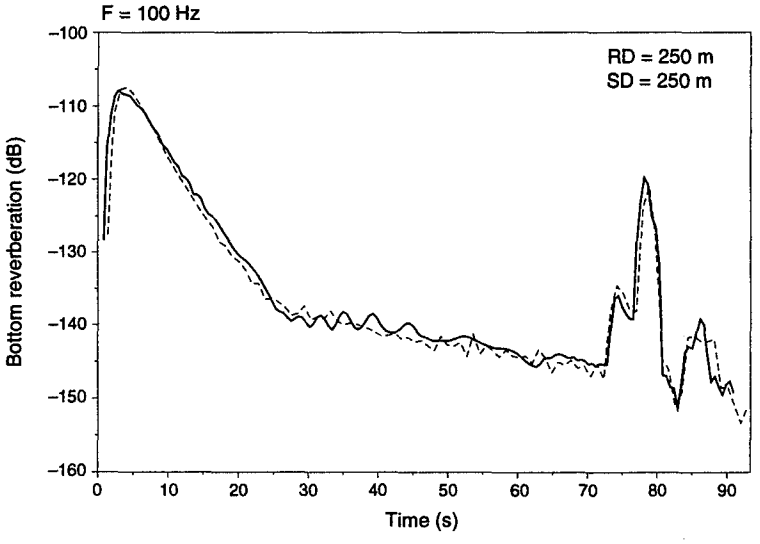

Figure 19 *Monostatic reverberation from the bottom – solid line (average of five frequencies) compared to the reverberation from MOCASSIN (dashed line).*

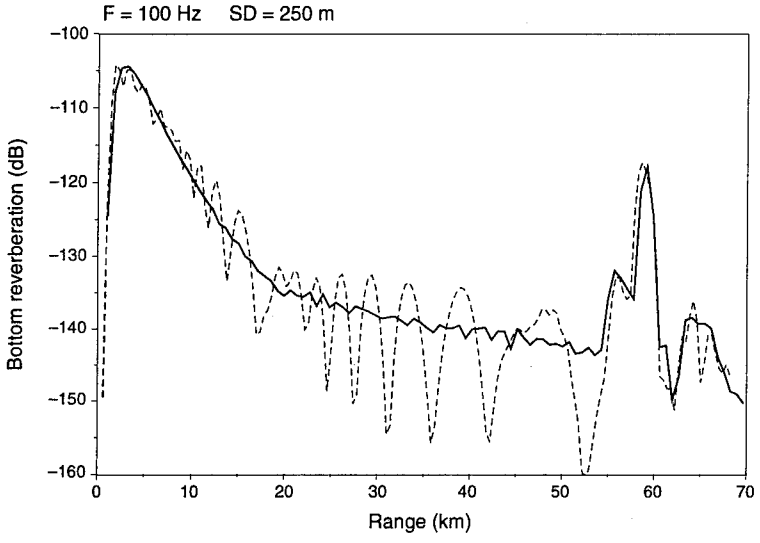

Figure 20 *Single frequency monostatic reverberation from the bottom (dashed line) compared to the reverberation from MOCASSIN (solid line).*

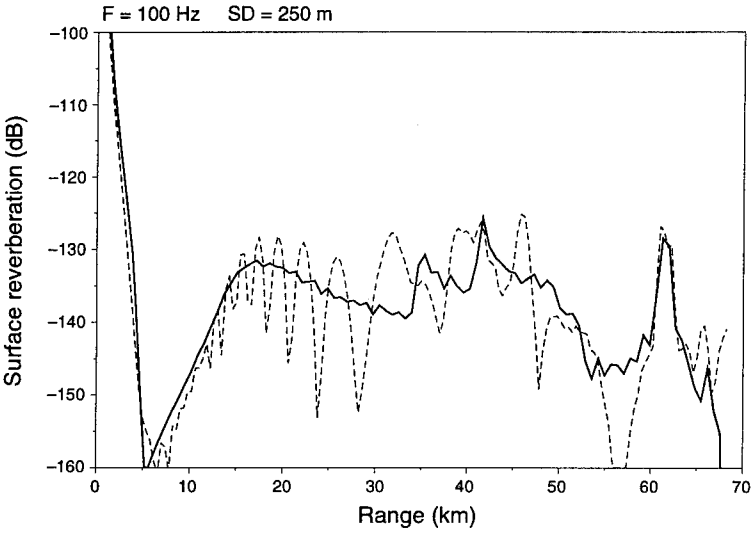

Figure 21 *Single frequency monostatic reverberation from the sea surface (dashed line) compared to the reverberation from MOCASSIN (solid line).*

4
Conclusion

The method of computing reverberation in a range-dependent environment developed earlier, has been extended from a monostatic geometry to allow for an arbitrary number of receiver depths. Two approaches have been pursued: one uses back-propagation and the second reciprocity of propagation. While giving the same reverberation results, the back-propagation approach is, in a realistic environment, more computer intensive and time consuming. This is because the backscattered field has to be propagated backwards from each reverberation element in range to the receiver position. The reciprocity approach is more flexible and can be used for few receiver depths which speeds up the computation considerably. Furthermore, it has proved quite easy to implement this reverberation option for arbitrary receiver depths into the standard PAREQ code which is now generally available.

References

[1] Schneider, H.G. Surface loss, scattering, and reverberation in the split-step parabolic wave equation model, SACLANTCEN SR-193. La Spezia, Italy, NATO SACLANT Undersea Research Centre, 1992. [AD B 171 009] Also: *Journal of the Acoustical Society of America*, **93**, 1993: 770–781.

[2] Jensen, F.B. and Martinelli, M.G. The SACLANTCEN Parabolic Equation model (PAREQ). La Spezia, Italy, NATO SACLANT Undersea Research Centre, 1985.

[3] Collins, M.D. and Evans, R.B. A two-way parabolic equation for acoustic backscattering in the ocean. *Journal of the Acoustical Society of America*, **91**, 1992: 1357–1368.

[4] Urick R.J. Principles of Underwater Sound. New York, NY, McGraw-Hill, 1975. [ISBN 0 07 066086 7]

[5] Weinberg, H. Generic Sonar Model, NUSC-TD-5971D. Newport, RI, Naval Underwater Systems Center, 1985. [AD B 095 689]

[6] Schneider, H.G. MOCASSIN – Sound Propagation and Sonar Range Prediction Model for Shallow Water Environments: User's Guide, FWG-TB-1990-9. Kiel, Germany, Forschungsanstalt der Bundeswehr für Wasserschall- und Geophysik, 1990.

Document Data Sheet

NATO UNCLASSIFIED

Security Classification		Project No.
NATO UNCLASSIFIED		19
Document Serial No.	**Date of Issue**	**Total Pages**
SR-225	November 1994	28 pp.

Author(s)

H.G. Schneider

Title

Vertically bistatic reverberation and the back-propagated field with the split-step PE

Abstract

This report continues the modelling of reverberation from the sea surface and the ocean bottom interface with the parabolic equation model PAREQ using the split-step algorithm. A previous report used the principle of propagation reciprocity to compute the reverberation for source and receivers which were co-located. Here the reverberation scheme is generalized to allow for differing depths of source and receiver, thus going from a monostatic to a 'quasi-bistatic' geometry. Additionally the full reverberant field is modelled by back-propagating the scatter contributions from the boundaries. This is done including geometrical spreading in azimuth, which requires the contributions from different ranges to be propagated independently. The back-propagated field is compared to solutions from two ray models (GSM, MOCASSIN) and displayed both as a function of range, i.e. equivalent to a transmission loss contour plot, and as a standard reverberation plot vs time.

Keywords

back-propagation, Generic Sonar Model, MOCASSIN, PAREQ, reverberation, vertically bistatic

Issuing Organization

North Atlantic Treaty Organization
SACLANT Undersea Research Centre
Viale San Bartolomeo 400, 19138 La Spezia, Italy

tel: 0187 540 111
fax: 0187 524 600
telex: 271148 SACENT I

[From N. America: SACLANTCEN CMR-426 (New York) APO AE 09613]

Initial Distribution for SR-225

Ministries of Defence	
DND Canada	10
CHOD Denmark	8
MOD France	8
MOD Germany	15
MOD Greece	11
MOD Italy	10
MOD Netherlands	12
CHOD Norway	10
MOD Portugal	5
MOD Spain	2
MOD Turkey	5
MOD UK	20
SECDEF US	54
NATO Authorities	
NAMILCOM	2
SACLANT	3
CINCIBERLANT	1
COMSUBACLANT	1
PAT	1
SCNR for SACLANTCEN	
SCNR Belgium	1
SCNR Canada	1
SCNR Denmark	1
SCNR Germany	1
SCNR Greece	1
SCNR Italy	1
SCNR Netherlands	1
SCNR Norway	1
SCNR Portugal	1
SCNR Spain	1
SCNR Turkey	1
SCNR UK	1
SCNR US	2
French Delegate	1
SECGEN Rep. SCNR	1
NAMILCOM Rep. SCNR	1
National Liaison Officers	
NLO Belgium	1
NLO Canada	1
NLO Denmark	1
NLO Germany	1
NLO Italy	1
NLO Netherlands	1
NLO UK	1
NLO US	1
Total external distribution	203
SACLANTCEN Library	22
Total number of copies	225